Carbon Nanotube-Based Thermoplastic Polyurethane-Poly (methyl methacrylate) Nanocomposites for Pressure Sensing Applications

Syed Muhammad Imran,[1,2] Godlisten N Shao,[1] M. Salman Haider,[1] Hae Jin Hwang,[3] Yong-Ho Choa,[1] Manwar Hussain,[1] Hee Taik Kim[1]

[1] *Department of Fusion Chemical Engineering, College of Engineering Sciences, Hanyang University, Ansan, Gyeonggi 426-791, Republic of Korea*

[2] *Department of Chemical Engineering, COMSATS Institute of Information Technology, Lahore, Pakistan*

[3] *School of Materials Science and Engineering, Inha University, Nam-Gu, Incheon 402-751, Korea*

We have synthesized unique flexible pressure-sensitive nanocomposites by means of a solution mixing method, by adding multiwalled carbon nanotubes (MWCNTs) into a thermoplastic urethane (TPU) matrix along with poly (methyl methacrylate) (PMMA) microbeads of various sizes. The influence of the various PMMA bead sizes on the pressure sensing properties of the nanocomposites was studied over a range of pressures. The PMMA microbeads were used to achieve an early percolation threshold at low loadings of MWCNTs. We used scanning electron microscopy to study the nanocomposites' morphology, and conducted differential scanning calorimetry analyses to investigate their thermal properties. The nanocomposites' electrical and thermal conductivities were also measured under various applied pressures. The nanocomposites displayed repeatable electrical responses under various applied pressures, demonstrating their suitability for use as pressure sensing materials. The proposed material is an ideal candidate for use in the preparation of pressure-sensitive devices. POLYM. ENG. SCI., 00:000–000, 2016. © 2016 Society of Plastics Engineers

INTRODUCTION

Carbon nanotubes (CNTs) are the most exciting thermally electroconductive nanomaterials discovered in recent years. Extensive studies have been conducted to investigate their unique properties, which include their high flexibility, low mass density, high aspect ratio, and extraordinary mechanical and electrical properties. They can also be used as an ideal reinforcing material to develop next-generation high-strength and multifunctional polymer nanocomposites [1, 2]. In recent years, researchers have focused on processing factors to yield high-quality nanocomposites with optimal properties. Key challenges faced by researchers in the case of CNTs are their poor dispersion in polymer matrices due to their high contact area, their random orientation, and the weak adhesion between the polymer and the CNTs, all of which affect the final properties of the nanocomposites [3, 4].

Thermoplastic polyurethanes (TPUs) are linear block copolymers characterized by alternating hard and soft segments. The hard segments are made from diisocyanate and the soft segments consist of long flexible polyether or polyester chains. In particular, the hard segments act as multifunctional tie points, working as both physical crosslinks and reinforcing fillers, whereas the soft segments primarily influence the elastic properties of the polymer [5]. TPUs exhibit many excellent properties such as high mechanical strength, good low-temperature flexibility, outstanding wear and abrasion resistance, and environmental resistance [6]. TPU show thermally and electrically insulating properties like most plastics, polymers, and rubbers. However, the introduction of a conductive material as filler in the polymer matrix can make it a conductive polymer. Such nanocomposites have wide range of applications such as in pressure sensors, antistatic devices, and electrical shielding [7, 8].

Including a low weight fraction of conductive filler in the polymer matrix will yield a highly resistive nanocomposite. The resistivity decreases with the increasing conductive filler content and finally drops by many orders of magnitude at a critical threshold [9–11]. Nanocomposites showing strong pressure-dependent resistivity can be used as pressure sensors. This phenomenon can be explained by the fact that when pressure is applied to these nanocomposites, percolation paths are formed within them, causing a sharp fall in resistivity even when the filler content is low. When pressure is applied to the nanocomposite, its total volume is reduced and thus the volume fraction of the filler effectively increases [12, 13].

The variation of electrical resistivity in polymer nanocomposites under varying pressure has been studied by many researchers in the last few years. Various researchers have reported the pressure dependence of resistivity for different nanocomposites. Hussain et al. [8, 9, 12] reported on the pressure dependence of resistivity for silicon rubber–carbon microball nanocomposites. They used a wet mixing method to prepare the nanocomposites, and these showed very good reproducibility in terms of pressure sensitivity. Rathod et al. [14] reported on the pressure sensing properties of TiO_2 doped with poly(vinyl alcohol) (PVA)/CN-Li at various temperatures and applied pressures. Wang et al. [15] studied the electrical resistance of flexible pressure-sensitive material based on carbon black-filled silicone nanocomposites. Shrivastava et al. [16] reported on the synthesis of poly(methyl methacrylate) (PMMA) by means of in situ bulk polymerization in the presence of multiwalled carbon nanotube (MWCNT) and commercial PMMA beads. They varied the size of the PMMA beads from 80 to 120 μm and used various bead contents

This article was published online on 3 June 2016. An error was subsequently identified in the author line. This notice is included in the online and print versions to indicate that both have been corrected 16 June 2016.

Correspondence to: H.T. Kim; e-mail: khtaik@yahoo.com and khtaik@hanyang.ac.kr or M. Hussain; e-mail: manwarh@hanyang.ac.kr

Contract grant sponsor: Korea Institute of Energy Technology Evaluation and Planning (KETEP) of the Ministry of Trade, Industry and Energy of the Republic of Korea, through its Human Resources Development Program; contract grant number: 20154030200680.

DOI 10.1002/pen.24333

Published online in Wiley Online Library (wileyonlinelibrary.com).

© 2016 Society of Plastics Engineers

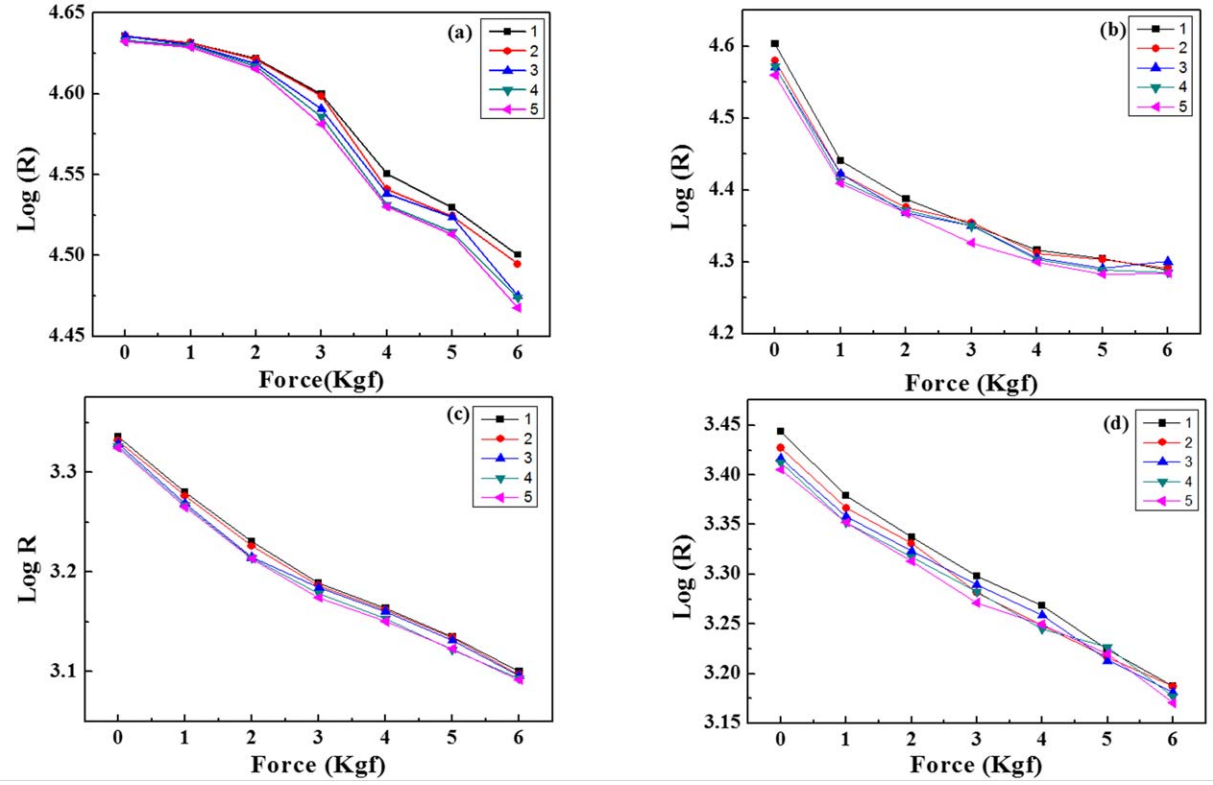


FIG. 1. Log of resistivity versus applied force for (a) TPU-CNT, (b) TPU-CNT-PMMA (5 μm), (c) TPU-CNTPMMA (10 μm), and (d) TPU-CNT-PMMA (20 μm). [Color figure can be viewed in the online issue, which is available at wileyonlinelibrary.com.]

(50, 60, 70, and 80 wt%) to achieve early percolation thresholds. However, they did not study the pressure sensing and thermal properties of the resulting nanocomposites. Gau et al. [17] reported the synthesis of polyamide-CNT nanocomposites by means of in situ polymerization and studied the composites' electrical resistivity under various pressures and temperatures. Kim et al. [18] coated PMMA beads with pristine MWCNTs to form nanocomposites and studied the electroconductive behavior of nanocomposites having various CNT contents.

In the present work, we used PMMA microbeads and MWCNTs in a TPU polymer matrix to create a segregated conductive network along the PMMA microbead grain boundaries, thereby achieving an early percolation threshold at a low loading of CNTs. PMMA microbeads of various sizes (i.e., 5, 10, and 20 μm) were added in 1 wt% loadings to TPU-MWCNT nanocomposites to study the effect of the PMMA microbead size upon the thermal and pressure sensing properties of the nanocomposites. They were also used to maintain mechano-elastic behavior of the nanocomposites. The resulting nanocomposites showed excellent sensing properties in response to changing external pressure, demonstrating their reliability for pressure sensing applications. Such a systematic evaluation of the effect of PMMA microbead size upon the thermal and pressure sensing properties of TPU-CNT nanocomposites has not previously been reported in the literature.

EXPERIMENTAL

Materials

All chemical reagents used in this study were of analytical laboratory grade and were used as received. TPU was procured from Austin Novel Materials, China. MWCNTs were purchased from Hanwha Nanotech Corp., South Korea. DMSO was purchased from Daejung Chemicals, South Korea. PMMA beads were purchased from Sunjin Chemicals, South Korea.

Synthesis of Nanocomposites

A solution mixing method was adopted to prepare the nanocomposites. A known amount of TPU was added to DMSO and stirred at 300 rpm at 50°C until it dissolved completely. In a

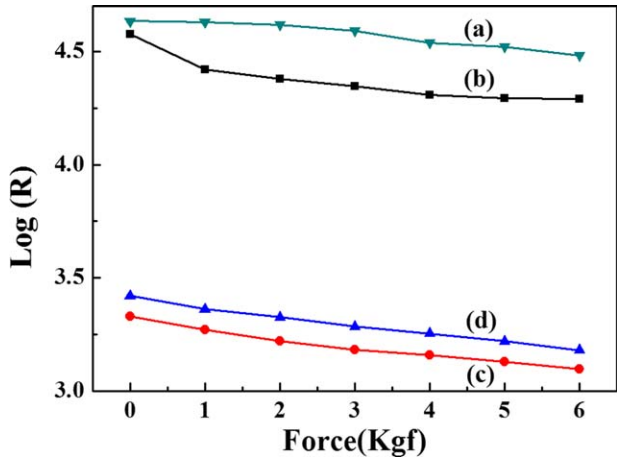


FIG. 2. Average log resistivity versus applied force for (a) TPU-CNT, (b) TPU-CNT-PMMA (5 μm), (c) TPUCNT-PMMA (10 μm), and (d) TPU-CNT-PMMA (20 μm). [Color figure can be viewed in the online issue, which is available at wileyonlinelibrary.com.]

DOI 10.1002/pen

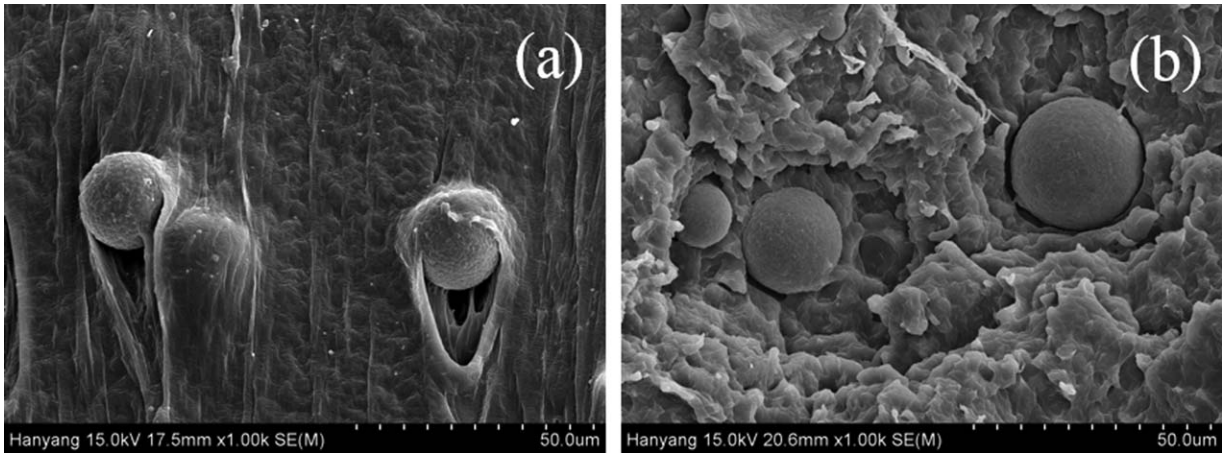


FIG. 3. SEM images of TPU-CNT-PMMA (20 μm), (a) under no external pressure and (b) under 6 kgf external pressure.

separate flask, CNTs (of 3.5 wt% relative to TPU) were added to DMSO and sonicated for 30 min to disaggregate them. The CNT solution was then added into the polymer solution and stirred for 12 hr to disperse the CNTs. Then, PMMA microbeads (of 1 wt% relative to TPU) of various sizes (5, 10, and 20 μm) were added to the nanocomposite solutions and stirred for 1 hr. The solutions were then removed from the stirrer and heated on a hot plate at 150°C to evaporate the DMSO. The resulting dried nanocomposites were removed and then formed into sheets by using a press molding machine (Auto M-NE, H 3891, Carver).

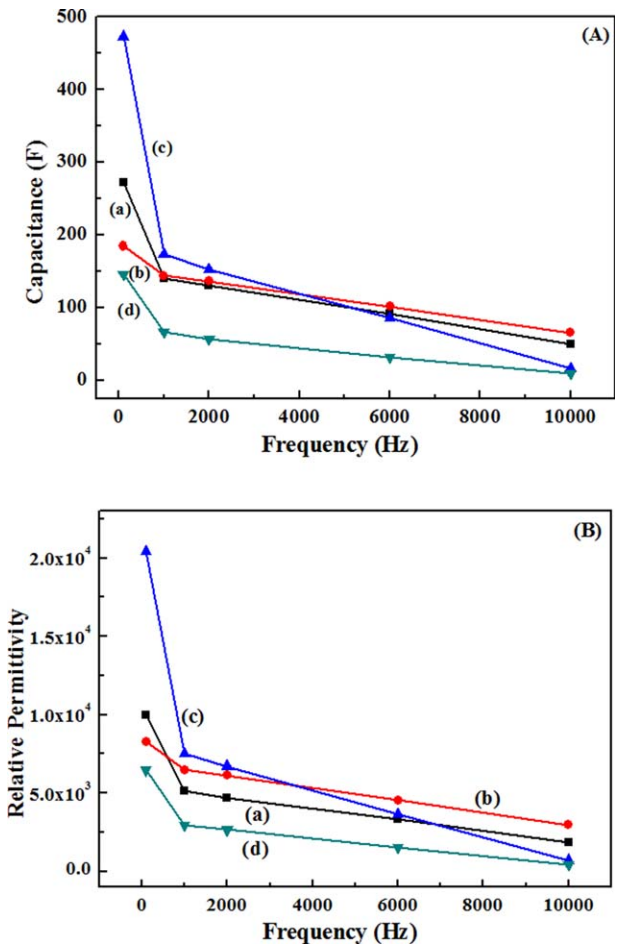


FIG. 4. Capacitance and relative permittivity of (a) TPU-CNT, (b) TPU-CNT-PMMA (5 μm), (c) TPU-CNTPMMA (10 μm) and (d) TPU-CNT-PMMA (20 μm). [Color figure can be viewed in the online issue, which is available at wileyonlinelibrary.com.]

Characterization

The electrical responses of the nanocomposites under various applied pressures were measured using a Metrotech tester operating at 220 V, 60 Hz, and 30 W (TC21206C, South Korea). Thermal conductivities were measured using a ThermalCon tester (MV 100PR, South Korea). Capacitance and relative permittivity values were measured using Hewlett Packard 4194A impedance analyzer (50 Ohms, Refurbished). Thermal properties were investigated by means of differential scanning calorimetry (DSC; Q2000 system, TA Instruments) conducted at the rate of 10°C/min under nitrogen. Sample morphologies were studied by

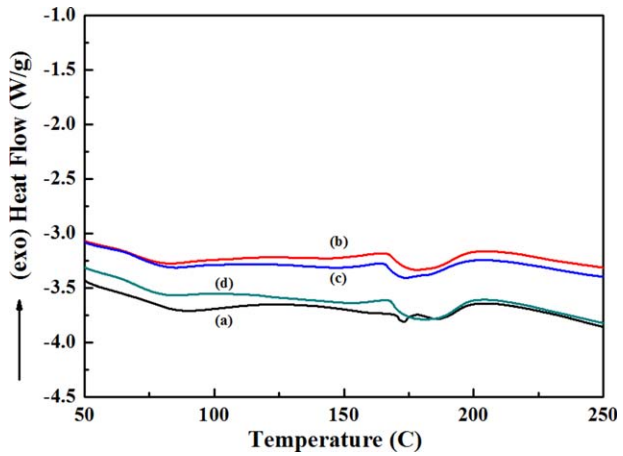


FIG. 5. DSC traces for (a) TPU-CNT, (b) TPU-CNT-PMMA (5 μm), (c) TPU-CNT-PMMA (10 μm) and (d) TPUCNT-PMMA (20 μm). [Color figure can be viewed in the online issue, which is available at wileyonlinelibrary.com.]

TABLE 1. Thermal properties of TPU-CNT-PMMA samples.

Sample	T_g (°C)	T_m (°C)	ΔH_m (J/g)	χ_c (%)
TPU-CNT	84	171.1, 183.6	0.84	8.43
TPU-CNT-PMMA (5 μm)	76.32	171.2, 182.2	0.68	8.1
TPU-CNT-PMMA (10 μm)	76.5	171.5, 181.6	0.67	8
TPU-CNT-PMMA (20 μm)	75.8	171.3, 181.2	0.64	7.7

Enthalpy of melting for TPU = ΔH_m (J/g) = 15.31 J/g.

means of scanning electron microscopy (SEM; JEOL JSM-6330F, Japan).

RESULTS AND DISCUSSION

PMMA microbeads of various sizes and MWCNTs were dispersed into TPU matrices to understand the effects of these additives' volume fractions upon the electrical and thermal conductivities of the resulting composites. Three such composites and a control composite not containing PMMA microbeads were each subjected to a sequence of five measurements in which the resistivity was measured while increasing the applied pressure. The composites showed considerable differences in the trend of falling resistivity with increasing external pressure (Fig. 1). It can be seen from the figures that there is a sharp decrease of resistivity with applied pressure in the region of 1 kgf pressure. However, after 2 kgf load the resistivity changes gradually. No large variations were observed among the five measurements, suggesting that this material is reliable for pressure sensing applications. When pressure of 1 kgf is applied to the nanocomposite, the CNTs come close to each other and form a three-dimensional conducting network; the pressure at which this occurs is known as a percolation threshold. PMMA microbeads present in the nanocomposites help to achieve contact among CNTs at low CNT loadings [9]. For the TPU-CNT nanocomposite without PMMA microbeads, the percolation threshold was ~3 kgf (Fig. 1a). For the nanocomposite with 5 μm PMMA microbeads, the percolation threshold was reduced to about 1 kgf (Fig. 1b). For the nanocomposites with larger microbeads of 10 and 20 μm, no clear percolation threshold was observed, but there was a gradual decrease in resistance (Fig. 1c and d); both these responses were linear, but some degradation in response was observed during repeated measurements of the latter sample.

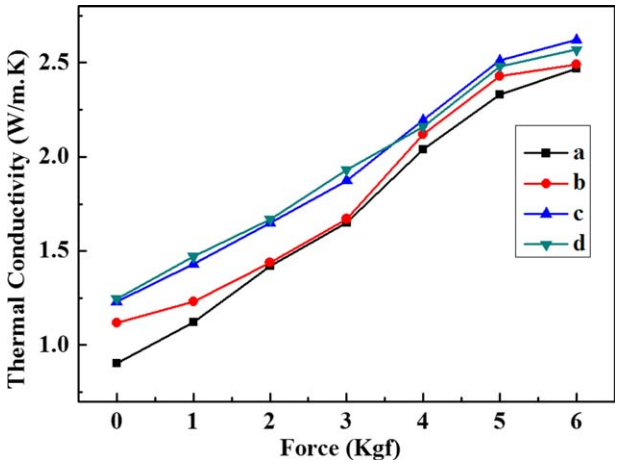


FIG. 6. Thermal conductivity versus applied pressure for nanocomposites with various PMMA bead sizes: (a) TPU-CNT, (b) TPU-CNT-PMMA (5 μm), (c) TPU-CNT-PMMA (10 μm), and (d) TPU-CNT-PMMA (20 μm). [Color figure can be viewed in the online issue, which is available at wileyonlinelibrary.com.]

Figure 2 shows the average log mean resistivity for the control TPU-CNT nanocomposite and those with PMMA microbeads of various sizes. The average log R value for the control TPU-CNT without any applied pressure was about 4.63 (Fig. 2a), whereas the addition of PMMA microbeads reduced the log R value to as low as 3.33 with the same CNT loading (Fig. 2c). This occurred because the PMMA microbeads occupy a certain volume in the polymer matrix, which can be regarded as an excluded volume that the CNTs cannot penetrate. Increasing this excluded volume increases the CNT concentration in the remaining volume of the polymer matrix, thereby increasing the composite's conductivity by bringing the CNTs closer to each other and allowing them to form conductive paths more easily [7, 16]. Notably, increasing the PMMA bead size from 5 to 10 μm reduced the resistivity, but increasing it further to 20 μm increased the resistivity slightly. This phenomenon was investigated by conducting SEM analysis of the nanocomposite including 20 μm PMMA beads.

In the absence of external pressure, the 20 μm PMMA beads were bonded to the polymer matrix, but this bonding broke under the applied pressure of 6 kgf (Fig. 3), thereby increasing the nanocomposite's electrical resistance. The decrease in conductivity for this nanocomposite could also have arisen partly from simple blockage in the conductive paths by the larger non-conductive microbeads.

Figure 4 shows the capacitance and relative permittivity of the prepared samples. All samples showed higher relative permittivity and capacitance values at low frequency and decreasing relative permittivity and capacitance with increasing frequency. The samples with 5 and 10 μm PMMA beads showed the highest relative permittivity and capacitance at various frequencies. There could be two possible explanations for this increase in relative permittivity and capacitance in case of 5 and 10 μm microbeads samples as compared to the samples with no microbeads and with 20 μm PMMA beads. The first reason could be due to the same mechanism that resulted in the high resistivity values of 20 μm as discussed in the curves of resistivity versus pressure of the nanocomposite samples (Figs. 1 and 2) and SEM results (Fig. 3). The second reason could be due to the accumulation of large amounts of interfacial charge at the interfaces between PMMA-CNT and TPU, which is known as the Maxwell–Wagner–Sillars (MW) effect [19–21].

Figure 5 shows DSC analysis results for the prepared samples; glass temperature (T_g), melting temperature (T_m), and enthalpy of melting (ΔH_m) data were obtained from the DSC traces and are listed in Table 1; the degree of crystallinity (χ_c) was calculated for each sample by using the formula $\chi_c = 100\% \times (\Delta H_m/\Delta H_m^0)/w$, where ΔH_m^0 is the enthalpy of melting for 100% crystalline TPU (15.31 J/g) [22] and w is the weight fraction of TPU in the sample. The addition of PMMA microbeads in the TPU-CNT nanocomposites resulted in the decrease in ΔH_m and χ_c. It is also important to note that ΔH_m and χ_c also decreased with increasing size of PMMA microbeads; this reduction of ΔH_m and χ_c in case of nanocomposites with respect to the neat polymers is generally observed when there are

DOI 10.1002/pen

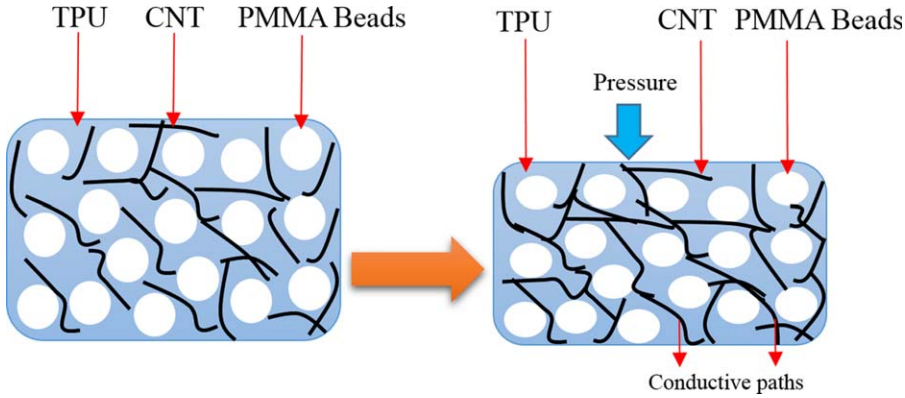


FIG. 7. Mechanism of the formation of conductive paths under pressure in TPU/CNT nanocomposites with PMMA beads. [Color figure can be viewed in the online issue, which is available at wileyonlinelibrary.com.]

specific interactions between the polymer components in the nanocomposites [23–25]. It was also noticed that T_m decreased slightly with the addition of PMMA microbeads. According to the Flory–Huggins theory, an increase in the melting temperature suggests an unfavorable interaction between the components, so the decrease in the melting temperature observed in the case of the TPU-CNT-PMMA nanocomposites indicated that the components may interact [26].

Figure 6 plots room-temperature measurements of thermal conductivity versus pressure for TPU-CNT nanocomposites with and without PMMA microbeads. There was a gradual increase in the thermal conductivity of the nanocomposites with increasing applied pressure up to 5 kgf; above this point, there was no significant increase in thermal conductivity in any of the nanocomposites tested, implying that most voids had been removed and the formation of conductive paths was mostly complete at 5 kgf. It can also be noted that the addition of PMMA microbeads of different sizes in the nanocomposites improved the thermal conductivities; among the nanocomposites tested, the one with 10 μm beads showed the greatest thermal conductivity. These results reinforce the resistivity results for the nanocomposites with the 10 μm PMMA microbeads, which showed no deviation and linear response in resistivity decrease with increasing pressure.

The mechanism whereby the PMMA microbeads allow lowering of resistance to be achieved at low CNT loadings is schematically illustrated in Figure 7. In a typical three-dimensional network structure, PMMA microbeads inside the TPU matrix occupy a certain volume, and when pressure is applied the total volume of the elastomer matrix decreases, thereby bringing the PMMA microbeads in the matrix closer to each other. This reduction in volume helps the CNT trapped between the PMMA microbeads and in the elastomer matrix to approach each other closely, even at low loadings, and to form conductive paths that allow electric current to pass through the matrix. Thus, enhanced electroconductive and pressure sensing properties can be achieved even at low filler loadings.

Based on these results it can be concluded that the presently proposed CNT-PMMA-based TPU nanocomposites can be used as reliable pressure sensing materials, and that the use of 10 μm PMMA beads in these nanocomposites is the best choice for the application, having yielded a very gradual decrease in resistance with increasing pressure and also having yielded the nanocomposite with the highest thermal conductivity among the bead sizes tested. Such electrical response of the nanocomposites with increasing pressure is important for their reliable application as pressure sensors.

CONCLUSIONS

TPU-CNT nanocomposites were prepared by means of a solution mixing technique. PMMA microbeads of different sizes (i.e., 5, 10, and 20 μm) were dispersed in the nanocomposite matrix in order to understand the effect of bead size upon the pressure dependence of the electrical and thermal conductivities in the resulting nanocomposites. When pressure was applied to the nanocomposites, CNTs present in the TPU matrix came close to each other and formed three-dimensional conducting network structures at the percolation threshold. PMMA microbeads present in the nanocomposites helped to achieve this contact between CNTs at low CNT loadings. The nanocomposites incorporating 10 μm beads showed the highest thermal conductivity; this phenomenon was explained by SEM analysis. DSC results confirmed possible interactions between the different components in the TPU matrix. Based on these results we can conclude that the nanocomposite with 10 μm bead size is the best choice for application as a pressure sensing material.

REFERENCES

1. A.K. Barick and D.K. Tripathy, *Mater. Sci. Eng., B*, **176**, 1435 (2011).
2. S. Scognamillo, E. Gioffredi, M. Piccinini, M. Lazzari, V. Alzari, D. Nuvoli, R. Sanna, D. Piga, G. Malucelli, A. Mariani, *Polymer*, **53**, 4019 (2012).
3. M. Wang, Y. Sun, X. Yang, and J. Zhao, *Food Chem.*, **179**, 318 (2015).
4. Y. Zare, *Synth. Met.*, **202**, 68 (2015).
5. P. Russo, M. Lavorgna, F. Piscitelli, D. Acierno, and L. Di Maio, *Eur. Polym. J.*, **49**, 379 (2013).
6. H. Li, N. Ning, L. Zhang, Y. Wang, W. Liang, M. Tian, T. W. Chan, *Polymer*, **67**, (2015).
7. N.K. Shrivastava and B.B. Khatua, *Carbon*, **49**, 4571 (2011).
8. M. Hussain, Y.H. Choa, and K. Niihara, *Script. Mater.*, **44**, 1203 (2001).
9. M. Hussain, Y.H. Choa, and K. Niihara, *Compos. A*, **32**, 1689 (2001).

10. E. Segal, R. Tchoudakov, M. Narkis, and A. Siegmann, *Polym. Eng. Sci.*, **42**, 2430 (2002).
11. S. Imran, Y. Kim, G. Shao, M. Hussain, Y. Choa, and H. Kim, *J. Mater. Sci.*, **49**, 1328 (2014).
12. M. Hussain, Y.H. Choa, and K. Niihara, *J. Mater. Sci. Lett.*, **20**, 525 (2001).
13. E. Segal, R. Tchoudakov, M. Narkis, and A. Siegmann, *J. Polym. Sci. Part B: Polym. Phys.*, **41**, 1428 (2003).
14. S.G. Rathod, R.F. Bhajantri, V. Ravindrachary, T. Sheela, P.K. Pujari, J. Naik, B. Poojary, *J. Polym. Res.*, **22**, 1 (2015).
15. L. Wang, F. Ma, Q. Shi, H. Liu, and X. Wang, *Sens. Actuators A*, **165**, 207 (2011).
16. N.K. Shrivastava, P. Kar, S. Maiti, and B.B. Khatua, *Polym. Int.*, **61**, 1683 (2012).
17. C. Gau, H.S. Ko, and H.T. Chen, *Nanotechnology*, **20**, 185503 (2009).
18. G. Kim, S. Kim, S.Y. Lee, M. Hussain, and Y.H. Choa, *J. Nanosci. Nanotechnol.*, **13**, 3936 (2013).
19. Y. Yao, N. Ning, L. Zhang, T. Nishi, and M. Tian, *RSC Adv.*, **5**, 23719 (2015).
20. G. Gallone, F. Carpi, D. De Rossi, G. Levita, and A. Marchetti, *Mater. Sci. Eng. C*, **27**, 110 (2007).
21. U. Tayfun, Y. Kanbur, U. Abaci, H.Y. Guney, and E. Bayramli, *Compos. B*, **80**, 101 (2015).
22. J.G. Drobny, Ed. *Handbook of Thermoplastic Elastomers*, PDL (Plastics Design Library)/William Andrew Pub., NY, 323 (2007).
23. V. Pistor, D. de Conto, F.G. Ornaghi, and A.J. Zattera, *J. Nanomater*, **2012**, 8 (2012).
24. M. Kashif, and Y.W. Chang, *Eur. Polym. J.*, **70**, 306 (2015).
25. J. Zhao, M. Chen, X. Wang, X. Zhao, Z. Wang, Z. Min Dang, L. Ma, G. Hua Hu, F. Chen, *ACS Appl. Mater. Interfaces*, **5**, 5550 (2013).
26. G.H. Lopes, J. Junges, R. Fiorio, M. Zeni, and A.J. Zattera, *Mat. Res.*, **15**, 698 (2012).

 DOI 10.1002/pen